Available online at www.sciencedirect.com
ScienceDirect
Journal of Power Sources 170 (2007) 419–424
JOURNAL OF POWER SOURCES
www.elsevier.com/locate/jpowsour

Short communication

Study the effects of mechanical activation on Li–N–H systems with ^{1}H and ^{6}Li solid-state NMR

Chun Lu [a,*], Jianzhi Hu [a], Ja Hun Kwak [a], Zhenguo Yang [a], Ruiming Ren [b,c], Tippawan Markmaitree [b], Leon L. Shaw [b]

[a] *Pacific Northwest National Laboratory, 902 Battelle Boulevard, Richland, WA 99352, USA*
[b] *Department of Materials Science and Engineering, University of Connecticut, Storrs, CT 06269, USA*
[c] *School of Materials Science and Engineering, Dalian Jiaotong University, Dalian 116028, China*

Received 29 December 2006; received in revised form 22 February 2007; accepted 23 February 2007
Available online 12 March 2007

Abstract

To gain insight into the effects of mechanical activation (MA) on the hydrogen desorption of the lithium amide ($LiNH_2$) and lithium hydride (LiH) mixture, $LiNH_2$ and $LiH + LiNH_2$ were mechanically activated by high-energy ball milling. The formed products were studied with in situ ^{1}H and ^{6}Li nuclear magic angle spinning (MAS) magnetic resonance (NMR) spectroscopy from ambient temperature to 180 °C. Up-field chemical shift was observed in ^{6}Li MAS NMR spectra with increased milling time, indicating that average local electronic structure around Li nuclei was modified during MA. ^{1}H MAS NMR was used to dynamically probe ammonia release from the activated $LiNH_2$ at temperature as low as 50 °C. In the case of activated $LiH + LiNH_2$ mixtures, the ^{1}H MAS NMR results implied that MA enhanced the dehydrogenation reaction of $LiNH_2 + LiH = Li_2NH + H_2$.

Keywords: Hydrogen storage; ^{1}H NMR; ^{6}Li NMR; Lithium amide and hydride; Chemical shift; Ammonia

1. Introduction

Li–N–H system, particularly lithium amide ($LiNH_2$) and lithium hydride (LiH) mixture, has been extensively investigated as potential hydrogen storage materials [1–17]. The dehydriding reaction of the system can be expressed as

$$LiNH_2 + LiH = Li_2NH + H_2 \quad (1)$$

with a theoretical reversible hydrogen storage capacity of 6.5 wt.%, which makes it very attractive for on-board storage applications. Although it is still debatable on the mechanism, it has been proposed that Reaction (1) proceeds with two elementary reactions [5], namely,

$$LiNH_2 = \tfrac{1}{2}Li_2NH + \tfrac{1}{2}NH_3 \quad (2)$$

followed by

$$\tfrac{1}{2}NH_3 + \tfrac{1}{2}LiH = \tfrac{1}{2}LiNH_2 + \tfrac{1}{2}H_2 \quad (3)$$

There exist at least a couple of technical barriers impeding practical application of the Li–N–H system. First, ammonia (NH_3), the intermediate product during H_2 formation from Reaction (2), can poison noble electrode catalysts of a fuel cell in the on-board system and also inevitably cause the storage-capacity decay. Secondly, the dehydriding reaction normally demands high temperature (~280 °C) to release H_2 at a pressure close to 1 bar because of sluggish kinetics [1–17]. To tackle these challenges, several strategies involving chemical and/or physical modification on the system have been pursued. For example, the system was modified via doped catalysts including Ni, Fe, Co, VCl_3, $TiCl_3$, TiO_2, Ti, Mn, MnO_2, V, and V_2O_5 [6,8,11,14], and/or partial substitution of Li with Mg having larger elelctronegativity to destabilize the metal–H bond in the amide to obtain improved kinetic and thermodynamic properties [7,8,11,12]. Lately, mechanical activation (MA) via high-energy ball milling was used to activate the Li–N–H systems with results clearly

* Corresponding author. Tel.: +1 509 375 6816; fax: +1 509 375 2186.
E-mail address: chun.lu@pnl.gov (C. Lu).

0378-7753/$ – see front matter © 2007 Elsevier B.V. All rights reserved.
doi:10.1016/j.jpowsour.2007.02.080

showing an improved kinetics for hydrogen release [6,11,16,17]. Although a variety of techniques including thermal analysis, scanning electron microscope, and X-ray diffraction provided useful knowledge in macroscopic to microscopic regime, the effects of MA on material properties for hydrogen storage at atomic level remains unclear.

Nuclear magnetic resonance (NMR), a non-invasive/non-destructive tool, is ideally suitable for real time in situ investigation of both the molecular structure and molecular dynamics at atomic level, provided that some practical concerns are properly addressed [18]. Due to a variety of inherent spin interactions in a solid, the NMR spectrum obtained from a static powder sample usually consists of many broad lines arising from chemically non-equivalent nuclei in a molecule [19–22]. This often results in a featureless spectrum and difficulty in interpretation. As for protons, major spin interactions include dipole–dipole interaction, chemical shift anisotropic interactions, and magnetic susceptibility interactions arising from variation of the magnetic susceptibility field near surfaces and boundaries. In a rigid solid, the dipole–dipole interactions alone can broaden a spectrum to as much as approximate 60 kHz [23]. In a hydrogen storage material, e.g. Li–N–H systems, hydrogen atom can exist at different states such as lattice-confined, surface adsorbed and gaseous. The lattice-confined is rigid, and consequently gives rise to very broad lines in the spectrum. The fast motion associated with surface adsorbed and gaseous hydrogen atom, in contrast, significantly averages the proton dipole–dipole and chemical shift interactions so that, in principle, a spectrum with narrow lines is expected. However, the synergy of residual dipole–dipole, chemical shift anisotropy interactions and magnetic susceptibility variations may still cause the spectral lines to broaden to such an extent that a high resolution ^{1}H NMR spectrum can hardly be yielded. To overcome the line broadening, however, magic angle spinning (MAS) solid-state NMR techniques were successfully developed and extensively applied for characterizing solid-state systems [18,20,23]. Thus, this work aims at (1) developing a MAS NMR method allowing high temperature characterization up to 180 °C; (2) consequently in situ studying the impact of mechanical activation on the properties of Li–N–H systems for hydrogen storage with ^{1}H and ^{6}Li MAS NMR.

2. Experimental

2.1. Sample preparation

Lithium amide with 95% purity was purchased from Alfa Aesar, while lithium hydride with 95% purity was purchased from Sigma–Aldrich. The $LiNH_2$ and LiH mixture was prepared with a molar ratio of 1–1.1 according to Reaction (1). The 10% excess of LiH was added to minimize the loss of NH_3 during the dehydriding process. In the case of amide, the as-received $LiNH_2$ was used. High-energy ball milling was conducted using a modified Szegvari attritor which had been shown previously to be effective in preventing the formation of the dead zone and producing uniform milling products within the powder charge [24]. Furthermore, a previous study has demonstrated that the seal of the canister of the attritor is air-tight and there is no oxidation during ball milling of LiH [25]. The canister of the attritor and balls 6.4 mm in diameter were both made of stainless steels. The loading of balls and the powder to the canister was performed in a glove-box filled with ultrahigh purity argon that contains Ar 99.999%, $H_2O < 1$ ppm, $O_2 < 1$ ppm, $H_2 < 3$ ppm, and $N_2 < 5$ ppm (referred to as Ar of 99.999% purity hereafter). The ball- to-powder weight ratio was 60:1, the milling speed was 600 rpm, and the milling temperature was maintained at 20 °C, achieved by water cooling at a flowing rate of 770 ml min^{-1}. Ball milling time was a variable in this study and adjusted from 45, 90 to 180 min.

2.2. NMR experiment

All NMR experiments were performed on a Varian-Chemagnetics 300 MHz Infinity spectrometer, corresponding to ^{1}H and ^{6}Li Larmor frequencies of 299.982 and 44.146 MHz, respectively. A commercial cross-polarization/MAS probe with a 7.5 mm outside diameter and 6 mm internal diameter pencil type spinner system was used. The sample cell resembles the commercial cell except that two solid Teflon plugs were made in such a manner that they can only be fully inserted into the zirconium cylinder after soaked into liquid nitrogen to seal ~0.1 g specimen. The specimen was first spun to the targeted spinning rate, i.e., 5.5 kHz ± 2 Hz using a commercial Chemagnetics MAS speed controller. For ^{6}Li MAS NMR, LiCl was the reference and each spectrum was acquired using a single pulse excitation sequence (~30° pulse width) with high power ^{1}H decoupling. A fixed number of accumulations were acquired at each temperature with a recycle delay time of 100 s for each spectrum. In the case of ^{1}H MAS (5.5 kHz) NMR, tetrakis(trimethylsilyl) silane (TKS), $[(CH_3)_3Si]_4Si$, was used as the reference, and spectra was acquired using a single 20° pulse excitation and a recycle delay time of 1 s plus an acquisition time of 0.2 s.

3. Results and discussion

3.1. Mechanically activated $LiNH_2$

The effects of mechanical activation on the ^{6}Li MAS NMR spectra at room temperature are shown in Fig. 1. Increasing milling time from 45 to 180 min causes a couple of noticeable changes in the spectra. Firstly, the full width at half maximum (FWHM) of the peak enlarges from 148 to 156 Hz, which indicates that the average local environment around Li nuclei becomes more disordered possibly due to structural refinements induced during MA. Since surface atoms experience surface relaxation and/or reconstruction compared with bulk atoms, the increased number of surface atoms could produce less-ordered state. This is consistent with the previous study in Ref. [16], revealing the increased surface area and number of surface defects induced by mechanical activation of $LiNH_2$. Secondly, the chemical shift of the peak position is up-field from 2.08 to 1.68 ppm. According to NMR principles, electrons circulating a nucleus shield the nucleus in a magnetic field. The more

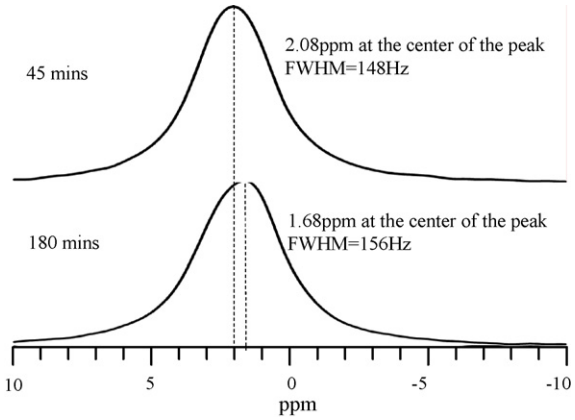

Fig. 1. Room temperature ^{6}Li MAS (5.5 kHz) NMR spectra of the $LiNH_2$ samples milled for 45 min (a) and 180 min (b), respectively.

shielding effect, the less effective magnetic field the nucleus experiences. Hence, low frequency (low energy) is required to excite the resonance so that the peak position shifts to the right in a spectrum [19–23]. Although the exact mechanism for triggering the up-field shift is still unknown, the result here clearly suggests that the average local electronic structure around Li nuclei changes when $LiNH_2$ was subjected to MA.

The ammonia releasing behavior of the 180 min milled $LiNH_2$ was probed dynamically at 50 °C and 40 consecutively acquired spectra are sequentially plotted in Fig. 2a. Each spectrum consists of a relatively sharp peak on the top of a broad peak. For illustration purpose, the 1st spectrum was zoomed out together with chemical shift scale in Fig. 2b. The broad peak originates from hydrogen in the rigid lattice of $LiNH_2$, and weak spinning side bands (SSBs) associated with the lattice hydrogen, as indicated by the arrows, are observed on the top of the broad peak at the sample spinning rate of 5.5 kHz. The sharp peak corresponds to the released NH_3 and it becomes higher with time. The intensity of the 40th spectrum is approximately 4.3 times of that of the 1st, while, in contrast, the intensity of the broad peak decreases with time. This is a strong indication of the dynamic conversion of the lattice protons in $LiNH_2$ to those in NH_3.

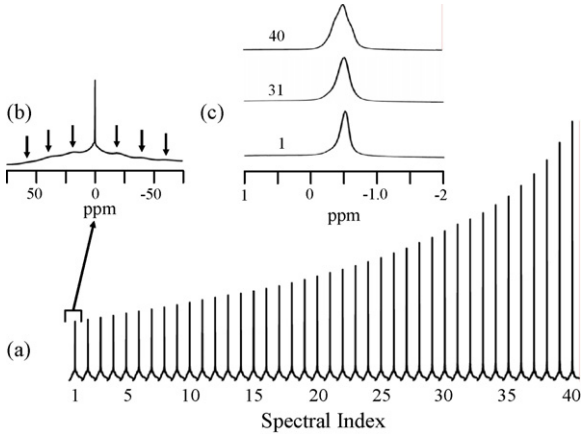

Fig. 2. ^{1}H MAS (5.5 kHz) NMR spectra of the 180 min milled $LiNH_2$ sample acquired at 50 °C: (a) ^{1}H NMR spectra as a function of time at 50 °C; (b) the enlarged plot of the 1st spectrum; (c) the expanded plots of the 1st, 31st and 40th spectra, highlighting the line shape changes for the narrow peak.

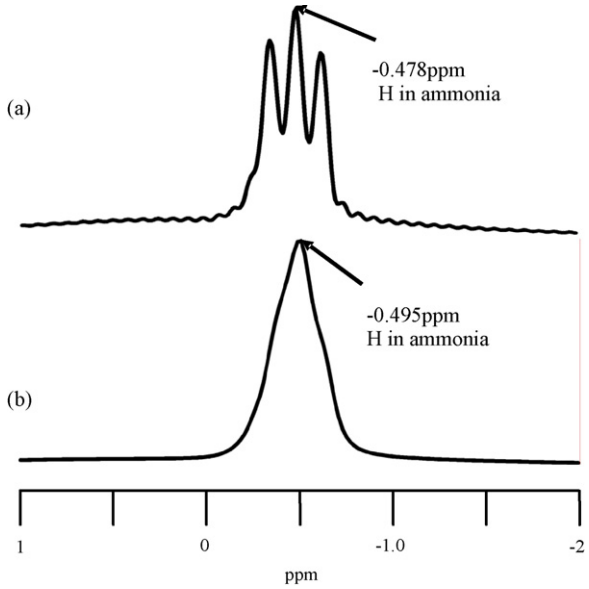

Fig. 3. Temperature dependence of ^{1}H MAS (5.5 kHz) NMR spectra of the $LiNH_2$ milled for 180 min, 75 °C (a) and 50 °C (b).

Fig. 2c shows expanded plots of the narrow peaks of the 1st, the 31st and the 40th spectra acquired at 50 °C, and shoulder peaks are noticeable along with the major peak centered at −0.478 ppm. In order to understand the origin of these peaks, the testing temperature was then increased to 75 °C and a spectrum was collected and is shown in Fig. 3 in which the 40th spectrum at 50 °C is included for comparison purpose. N–H *J*-coupling with a coupling constant of approximately 43 Hz in NH_3 is observed at 75 °C, which is originated from the coupling of electron orbital between N and H atoms. The *J*-coupling effect causes the peak to split into three sharp peaks centered at −0.478 ppm since ^{14}N (99.635% natural abundance) has spin quantum of 1. The sharp peaks also imply that the corresponding NH_3 molecules experience fast molecular motion, indicating the presence of gaseous ammonia. Contrast to this, the spectrum at 50 °C appears to have broader peaks centered at −0.495 ppm, suggesting limited mobility for the protons in ammonia. Because the *J*-coupling effect is not strongly temperature dependent, one would expect the similar effect if gaseous phase ammonia exists at 50 °C. Consequently, most of the detected ammonia at 50 °C is likely confined by the surface probably through adsorption, which is consistent with thermal analysis characterization [17]. In addition, low intensities of the *J*-coupling peaks in the spectra with index number below 31st, as shown in Fig. 2c, hint that the kinetics of the generation of the surface-confined ammonia at 50 °C is relatively sluggish. Nevertheless, the ammonia generated at 50 °C from $LiNH_2$ with 180 min ball milling has been shown to be about 820 times that produced by $LiNH_2$ without MA [16].

3.2. *Mechanically activated $LiNH_2$ + LiH mixtures*

The ball milled $LiNH_2$ + LiH mixtures were subjected to ^{6}Li MAS NMR measurement at room temperature (RT) and 180 °C, and the spectra are summarized in Fig. 4. The peaks correspond-

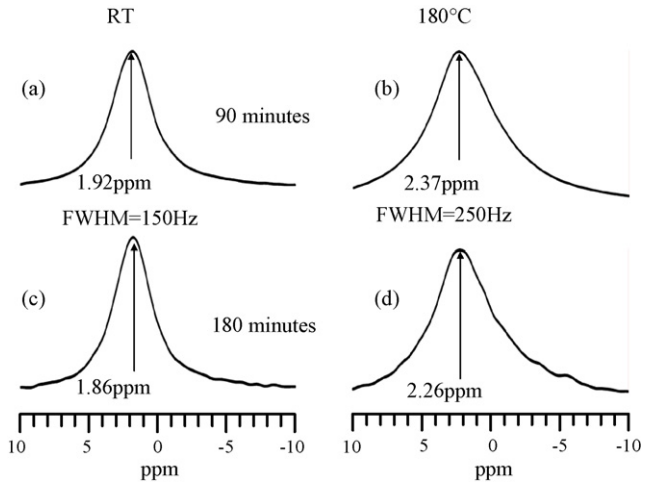

Fig. 4. ^{6}Li MAS (5.5 kHz) NMR spectra for the $LiNH_2$ + LiH milled for 90 min (a and b) and 180 min (c and d), respectively.

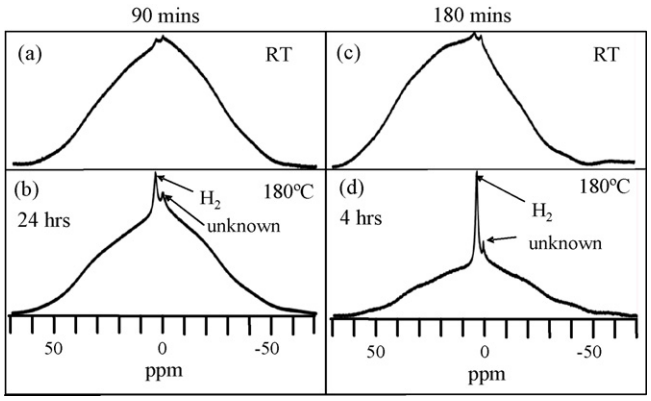

Fig. 6. ^{1}H MAS (5.5 kHz) NMR spectra of LiH + $LiNH_2$ mixtures as a function of temperature (RT vs.180 °C) and milling time (90 min vs. 180 min): (a) 90 min ball milling and acquired at RT; (b) 90 min ball milling and acquired 24 h after the temperature reaches 180 °C; (c) 180 min ball milling and acquired at RT; (d) 180 min ball milling and acquired 4 h after the temperature reaches 180 °C.

ing to the lithium in LiH and $LiNH_2$ are overlapped due to the relatively large line widths and the small chemical shift difference of only about 0.61 ppm, as shown in Fig. 5. Thus, only one peak can be identified in Fig. 4. At both RT and 180 °C the peak center position is up-field shifted when milling time increased from 90 to 180 min. For instance at RT the peak position shift from 1.92 to 1.86 ppm, while from 2.37 to 2.26 ppm at 180 °C. Although the up-field magnitude is not as significant as that observed in the case of $LiNH_2$, the results here still suggest the change of average local electronic structure around Li nuclei during MA.

^{1}H MAS NMR was used to examine hydrogen production from the mechanically activated LiH + $LiNH_2$ mixtures. Fig. 6 displays the spectra measured at room temperature and 180 °C for the LiH + $LiNH_2$ milled for 90 and 180 min, respectively. Since these two samples were prepared and characterized under identical conditions, the NMR results can be comparatively analyzed. Again, the broad peak arises from the rigid lattice protons. Tiny sharp peaks at room temperature suggest the existence of hydrogen, which agrees with the TGA and DSC characterization results reported previously [17]. When temperature increased to 180 °C, two sharp peaks become more distinguishable with one at ~4.06 ppm and the other at ~1.06 ppm. The peak at ~4.06 ppm is assigned to H_2 based on previously reported chemical shifts for H_2 [26,27], and the origin for the other peaks remains unclear and requires further investigation. These assignments are also highlighted in Fig. 7 where only the spectra ranging from −5 to 10 ppm are plotted. For the

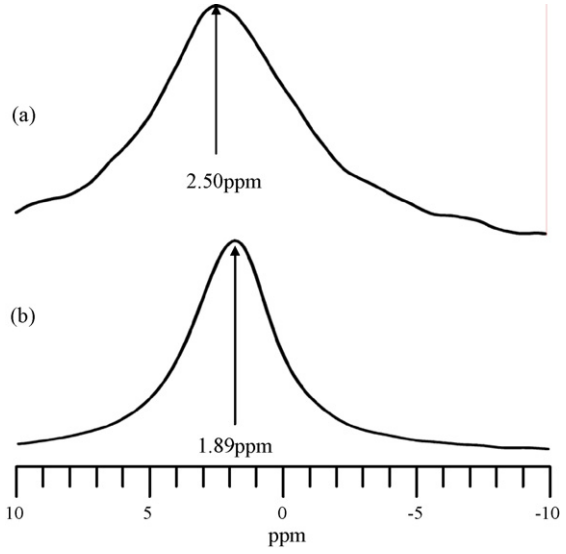

Fig. 5. Room temperature ^{6}Li MAS NMR spectra for the LiH (a) and $LiNH_2$ (b).

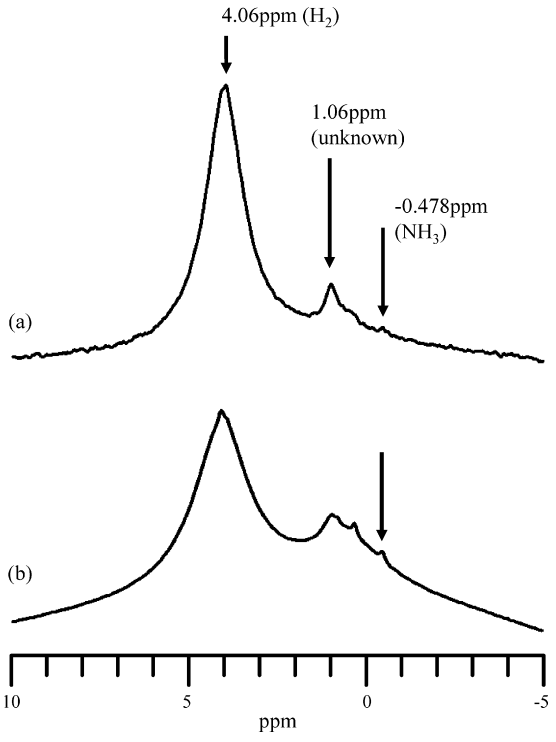

Fig. 7. ^{1}H MAS (5.5 kHz) NMR spectra of LiH + $LiNH_2$ mixtures: (a) the expanded plot of the spectrum in Fig. 5d; (b) the expanded plot of the spectrum in Fig. 5b.

180 min milled sample, the spectrum was collected after stabilizing the temperature at 180 °C for 4 h, while for the 90 min milled sample the spectrum was recorded after 24 h at 180 °C. The relative height of the H_2 peak spurring out from the broad peak is much larger for the 180 min milled specimen, which implies that long-time MA enhances the dehydrogenation from $LiNH_2 + LiH = Li_2NH + H_2$. In addition, the relative integrated ratio of the NH_3 peak of the 180 min milled sample is apparently lower than that in the 90 min milled sample, which implies that long-time MA also probably suppresses the ammonia generation. Compared with the spectrum in Fig. 2c, the ammonia peak in Fig. 7 is substantially reduced and H_2 peak becomes dominant with the presence of LiH. This observation in part supports the reaction mechanism shown by Reactions (2) and (3) in which ammonia is involved as the intermediate specie for hydrogen release from $LiH + LiNH_2$ mixtures.

The hydrogen release from the 180 min milled sample was continuously monitored with ^1H MAS NMR at 180 °C. Total 40 spectra were consecutively recorded and are plotted in Fig. 8a. The 1st and 40th spectra ranging from −5 to 10 ppm are separately shown in Fig. 8b and c, respectively. The line width, defined as the full width at half height peak (FWHM) positions, changes from 415 Hz (b) to 342 Hz (c). Such a line narrowing indicates increased mobility of the generated H_2. Likely the produced H_2 initially adsorbs on the surface of the solid mixtures prior to forming gaseous H_2. Due to the restricted molecular motion from the surface-adsorbed H_2, the NMR spectrum shows a broad line width. As time increases, the line width decreases because of the large mobility of accumulated H_2 in gaseous state in the sample holder. Also the peak height increases initially and then tends to level off gradually. This trend suggests that the gas pressure of H_2 gradually approaches the equilibrium value within the closed sample cell, which is consistent with the expectation of the reversible reactions as shown in Reaction (1) or Reactions (2) and (3).

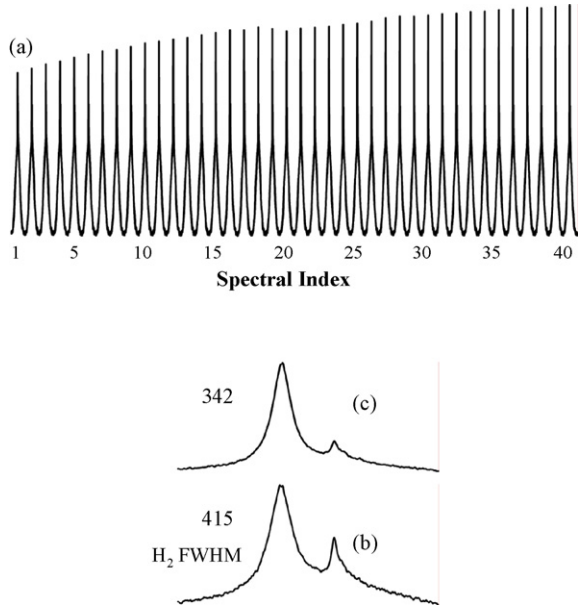

Fig. 8. (a) ^1H MAS (5.5 kHz) NMR spectra of the 180 min milled $LiH + LiNH_2$ sample as a function of time at 180 °C. The 1st spectrum (b) and the 40th spectrum (c).

4. Conclusions

^1H and ^6Li MAS NMR spectroscopy is a powerful tool to in situ study hydrogen storage materials, and is used to examine the influence of mechanical activation on the properties of hydrogen production from $LiNH_2$ and $LiH + LiNH_2$ mixtures. The results suggest that mechanical activation leads to the change of local electronic structure around Li nuclei and also causes structural refinements. In the case of MA $LiNH_2$, ammonia was detected and dynamically probed at 50 and 75 °C with ^1H MAS NMR. The hydrogen release properties of the milled $LiH + LiNH_2$ mixtures were studied at 180 °C. NMR analysis suggests that mechanical activation strongly enhances hydrogen desorption.

Acknowledgements

This work was supported under the U.S. Department of Energy (DOE) Contract No. DE-FC36-05GO15008. The research was performed in the Environmental Molecular Sciences Laboratory (a national scientific user facility sponsored by the Department of Energy's Office of Biological and Environmental Research) located at PNNL, and operated for DOE by Battelle under Contract No. DE-AC05-76RL01830.

References

[1] P. Chen, Z. Xiong, J.Z. Luo, J.Y. Lin, K.L. Tan, Nature 420 (2002) 302–304.
[2] P. Chen, Z. Xiong, J.Z. Luo, J.Y. Lin, K.L. Tan, J. Phys. Chem. B 107 (2003) 10967–10970.
[3] Y.H. Hu, E. Ruckenstein, Ind. Eng. Chem. Res. 42 (2003) 5135–5139.
[4] Y.H. Hu, E. Ruckenstein, J. Phys. Chem. A 107 (2003) 9737–9739.
[5] T. Ichikawa, N. Hanada, S. Isobe, H. Leng, H. Fujii, J. Phys. Chem. B 108 (2004) 7887–7892.
[6] T. Ichikawa, S. Isobe, N. Hanada, H. Fujii, J. Alloys Compd. 365 (2004) 271–276.
[7] S. Orimo, Y. Nakamori, G. Kitahara, K. Miwa, N. Ohba, T. Noritake, S. Towata, Appl. Phys. A 79 (2004) 1765–1767.
[8] T. Ichikawa, N. Hanada, S. Isobe, H. Leng, H. Fujii, Mater. Trans. 46 (2005) 1–14.
[9] Y. Kojima, Y. Kawai, J. Alloys Compd. 395 (2005) 236–239.
[10] Y.H. Hu, E. Ruckenstein, Ind. Eng. Chem. Res. 43 (2004) 2464–2467.
[11] J.H. Yao, C. Shang, K.F. Aguey-Zinsou, Z.X., Guo, J. Alloys Compd., in press.
[12] H.Y. Leng, T. Ichikawa, S. Isobe, S. Hino, N. Hanada, H. Fujii, J. Alloys Compd. 404–406 (2005) 443–447.
[13] G.P. Meisner, F.E. Pinkerton, M.S. Meyer, M.P. Balogh, M.D. Kundrat, J. Alloys Compd. 404–406 (2005) 24–26.
[14] S. Isobe, T. Ichikawa, N. Hanada, H.Y. Leng, M. Fichtner, O. Fuhr, H. Fujii, J. Alloys Compd. 404–406 (2005) 439–442.
[15] T. Ichikawa, N. Hanada, S. Isobe, H.Y. Leng, H. Fujii, J. Alloys Compd. 404–406 (2005) 435–438.
[16] L.L. Shaw. R. Ren, T. Markmaitree, W. Osborn, J. Alloys Compd., in press.
[17] T. Markmaitree, R. Ren, L.L. Shaw, J. Phys. Chem. B 110 (2006) 20710–20817.
[18] K.D.J. Mackenzie, M.E. Smith, Multinuclear Solid-State NMR of Inorganic Materials, Pergamon, An Imprint of Elsevier Science, 2002.

[19] M.H. Levitt, Spin Dynamics: Basics of Nuclear Magnetic Resonance, John Wiley & Sons Ltd., 2001.
[20] K. Schmidt-Rohr, H.W. Spiess, Multidimensional Solid-State NMR and Polymers, Academic Press, 1994.
[21] A. Abragam, The Principles of Nuclear Magnetism, Oxford University Press, London, 1961 (Chapter V).
[22] C.P. Slichter, Principles of Nuclear Magnetic Resonance, third ed., Springer, Berlin, 1990.
[23] B.C. Gerstein, C.R. Dybowsky, Transient Techniques in NMR of Solids, Academic Press, San Diego, 1985.
[24] Z.-G. Yang, L. Shaw, Nanostruct. Mater. 7 (1996) 873–886.
[25] R. Ren, A.L. Ortiz, T. Markmaitree, W. Osborn, L. Shaw, J. Phys. Chem. B 110 (2006) 10567–10575.
[26] M. Shiraishi, M. Ata, J. Nanosci. Nanotech. 2 (2002) 463–465.
[27] Q. Zeng, J.F. Stebbins, A.D. Heaney, T. Erdogan, J. Non-Cryst. Solids 258 (1–3) (1999) 78–91.